

# Vapor-Liquid Phase Behavior of the Helium-Methane System

J. E. SINOR, D. L. SCHINDLER, and FRED KURATA

University of Kansas, Lawrence, Kansas

This report presents more extensive experimental vapor-liquid equilibria data for the helium-methane system than are found in the literature. A static sampling technique was used to obtain vapor and liquid compositions for six temperatures between  $-180^{\circ}$  and  $-85^{\circ}\text{C.}$  and pressures up to 2,000 lb./sq.in.abs. Data at 2,000 lb./sq.in.abs. were extended to the critical temperature of the mixture.

Average scatter of the data from the smoothed lines is approximately 1% of the helium concentration or 0.03 mole % helium, whichever is larger. Vapor compositions at  $-140^{\circ}$ ,  $-160^{\circ}$ , and  $-180^{\circ}\text{C.}$  were analyzed by a different technique and scattered on the average from the smoothed curve less than 4% of the methane concentration. Comparisons are drawn between the data of this study and the previously published work of Kharakhorin. The solubility of helium in liquid methane was found to be considerably less than the values indicated by Kharakhorin.

Experimental data are presented in tabular form and in various phase composition diagrams. The behavior of the helium-methane system is seen to be very similar to that of the helium-nitrogen system, with helium being much less soluble in methane than in nitrogen.

The data were satisfactorily represented by means of the Krichevsky-Kazarnovsky equation. Extrapolations to higher pressures should be feasible.

Interest in conserving the only appreciable supply of helium has led to legislation enabling private industry to extract helium from streams of natural gases in which it occurs. The helium is purchased by the government for storage in underground formations. The separation processes used by all recovery plants now in operation depend upon low-temperature phase equilibrium phenomena. Since helium is the least condensible of all gases, it is obtained by condensing all of the other components present in the natural gas. The helium-free natural gas is then returned to the market stream.

The efficiency of the low-temperature recovery process is affected by loss of helium dissolved in the condensed natural gas returning to the pipeline, and in the liquid nitrogen which condenses in the final purification step. A number of investigators have published studies of the solubility of helium in liquid nitrogen (1 to 6, 10). The solubility of helium in liquified hydrocarbons, however, has received very little attention. Some data concerning the solubility of helium in certain specific natural gas mixtures have been provided by the United States Bureau of Mines.

Only two articles can be found in the general literature containing data for the helium-methane binary system. Gonikberg and Fastovskii (5) determined liquid phase data only for isotherms of  $-182.9^{\circ}$  and  $-167.2^{\circ}\text{C.}$  at pressures up to 2,350 lb./sq. in. abs. Kharakhorin (7) investigated the vapor-liquid equilibria at temperatures of  $-182.1^{\circ}$ ,  $-161.7^{\circ}$ ,  $-136.2^{\circ}$ , and  $-122.9^{\circ}\text{C.}$  and pressures up to 2,450 lb./sq. in. abs. Since the two studies do not share any common isotherms or isobars, it is impossible to make a direct comparison of the data. However, by interpolating at even pressures on a pressure-composition diagram and then plotting temperature vs. composition at constant pressure, the data from these two sources are seen to be quite inconsistent. Kharakhorin's data indicate a higher solubility of helium in liquid methane. The present study was undertaken to resolve the inconsistency and to extend the data over a wider temperature range.

J. E. Sinor is with Rocketdyne, Canoga Park, California.

## EXPERIMENTAL

Figure 1 is a schematic of the experimental cell and sampling manifold. Gas is introduced at *H*, and after two-phase equilibrium is established, vapor and liquid samples are drawn off for analysis through lines *J* and *K*, respectively. The valves *C* and *F* are outside the low-temperature bath containing the cell. The cell itself is made of brass and the agitator *G* of 417 stainless steel. The line connections and all internal joints at the top of the cell are silver brazed to provide leak-proof

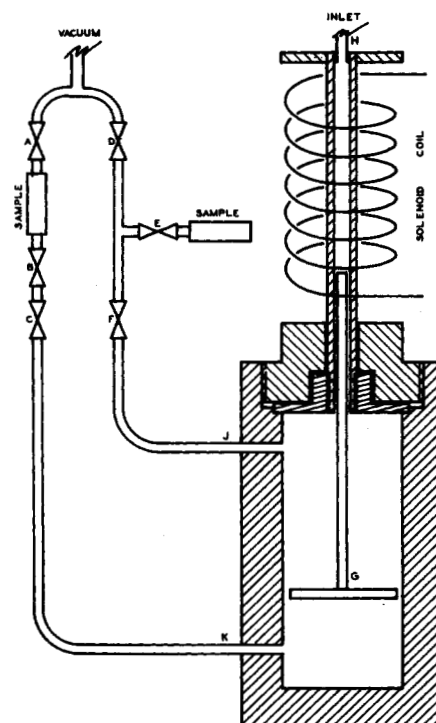


Fig. 1. Equilibrium cell and sampling manifold.

TABLE 1. EXPERIMENTAL VAPOR-LIQUID EQUILIBRIUM DATA.  
HELIUM-METHANE SYSTEM

Temperature, °C.	Pressure, lb./sq. in. abs.	Liquid composition, mole % helium	Vapor composition, mole % helium
-85	620	0	0
	750	1.49	5.8
	1,000	4.28	16.9
	1,250	6.78	25.3
	1,500	9.06	32.2
	1,750	11.05	37.2
-100	2,000	13.00	41.5
	385	0	0
	500	0.60	15.0
	750	1.89	36.1
	1,000	3.22	49.1
	1,250	4.17	55.4
-120	1,500	5.24	63.2
	1,750	6.18	67.4
	2,000	7.12	71.3
	180	0	0
	400	0.58	51.9
	600	1.09	66.7
-140	800	1.63	74.4
	1,000	2.05	—
	1,250	2.66	82.5
	1,500	3.20	85.0
	1,750	3.66	86.7
	2,000	4.04	88.4
-160	66	0	0
	250	0.24	69.6
	500	0.56	83.7
	750	0.86	—
	1,000	1.16	91.2
	1,250	1.44	—
-180	1,500	1.69	93.8
	1,750	1.93	—
	2,000	2.14	95.2
	18	0	0
	250	0.13	91.4
	500	0.28	95.7
-180	750	0.42	96.9
	1,000	0.55	97.6
	1,250	0.67	98.0
	1,500	0.78	98.2
	1,750	0.90	98.4
	2,000	0.99	98.5
-180	3	0	0
	250	0.06	98.4
	500	0.11	99.2
	750	0.16	99.4
	1,000	0.22	99.5
	1,250	0.26	—
-180	1,500	0.32	99.7
	1,750	0.34	—
	2,000	0.39	99.8

construction. The internal volume of the cell is approximately 100 cc.

Agitation of the cell contents in order to bring the system to thermodynamic equilibrium is accomplished by momentarily applying an alternating current voltage to the solenoid coil which raises the plunger G. When the current is interrupted, the plunger drops by gravity. Continuous agitation is provided by a small motor driving a cam which briefly closes, then opens a microswitch in the line supplying the coil voltage. The switch is closed approximately once every second.

The sample lines J and K are made of stainless steel capillary tubing with an O.D. of  $\frac{1}{8}$  in. and an I.D. of 0.023 in. The tubing is then filled with 0.018-in. diameter music wire to reduce dead volume. The sampling valves are needle valves with tubing fittings, chosen for their small dead volume. The ends of the sample lines are machined so as to extend into the

valve body and occupy most of the dead volume originally present in the valves. The entire volume between the cell and the valve seat of valves C and F is less than 0.1 cc each.

The sample bulbs are short lengths of  $\frac{1}{8}$  in. I.D. stainless steel tubing. Total sample volume is approximately 0.5 cc. Samples were analyzed by gas chromatography. The accuracy of the analyses is  $\pm 0.03$  mole % helium, or  $\pm 1.0\%$  of the helium concentration, whichever is larger. Because of the extremely low methane concentration in the vapor phase at low temperatures, vapor compositions on the  $-140^\circ$ ,  $-160^\circ$ , and  $-180^\circ$  C. isotherms were determined by direct measurement of the methane concentration on the gas chromatograph. Helium carrier gas and a large sampling loop were used to increase the sensitivity of the analysis. The data scattered from the smoothed curve on the average less than 4% of the methane concentration.

Temperatures inside the low-temperature bath were measured with a platinum resistance thermometer. This thermometer was calibrated against another thermometer which had been compared with a National Bureau of Standards standard. The calibration is believed to be within  $0.02^\circ$  C. This thermometer also served as the sensing element for the temperature control system. The bath fluid was air, circulated at high velocity. Temperature fluctuations within the bath were less than  $0.01^\circ$  C.

Pressures were measured with Bourdon tube gauges, which had been calibrated against a dead weight tester. All reported pressures are believed to be accurate to within  $\pm 1.5$  lb./sq. in.

To begin a run, the cell was evacuated and the bath brought to the desired temperature. Enough methane was admitted to fill the cell approximately half full with liquid. The system was then pressurized with helium and when the desired pressure was reached, the agitator motor was started. As helium dissolves in the liquid phase during agitation, the system pressure drops and more helium must be added to maintain constant pressure.

Equilibrium was indicated when the system pressure reached a constant value. The system was usually agitated for 5 min. and then allowed to remain quiescent for 15 min., the alternations being continued for at least 1 hr. The pressure seldom changed after the first 5 min. of agitation, indicating a high efficiency of mixing within the cell.

After reaching steady state equilibrium, the sample lines were flushed and samples withdrawn from the system. Regardless of which phase was sampled first, the system was agitated and again brought to equilibrium pressure before drawing the second sample. A new point along the isotherm was then approached by either increasing or decreasing the system pressure. In all data runs some of the points on every isotherm were obtained by increasing pressure steps and some by decreasing pressure steps.

The helium used in this study was a special analyzed stock furnished by the U. S. Bureau of Mines and had a maximum impurity of 12.0 p.p.m. The methane was "pure grade" supplied by Phillips Petroleum Company with a minimum purity of 99 mole %.

TABLE 2. EXPERIMENTAL VAPOR-LIQUID EQUILIBRIUM DATA.  
TEMPERATURES AND COMPOSITIONS ALONG THE  
2,000 LB./SQ. IN. ABS. ISOBAR

Temperature, °C.	Liquid composition, mole % helium	Vapor composition, mole % helium
-180.0	0.39	99.8
-160.0	0.99	98.5
-140.0	2.14	95.2
-120.0	4.04	88.4
-100.0	7.12	71.3
-85.0	13.0	41.5
-84.0	13.8	37.2
-83.5	15.2	34.8
-83.0	16.6	32.0
-82.7	17.8	30.0
-82.5	18.3	28.7
-82.2	26.5	27.5

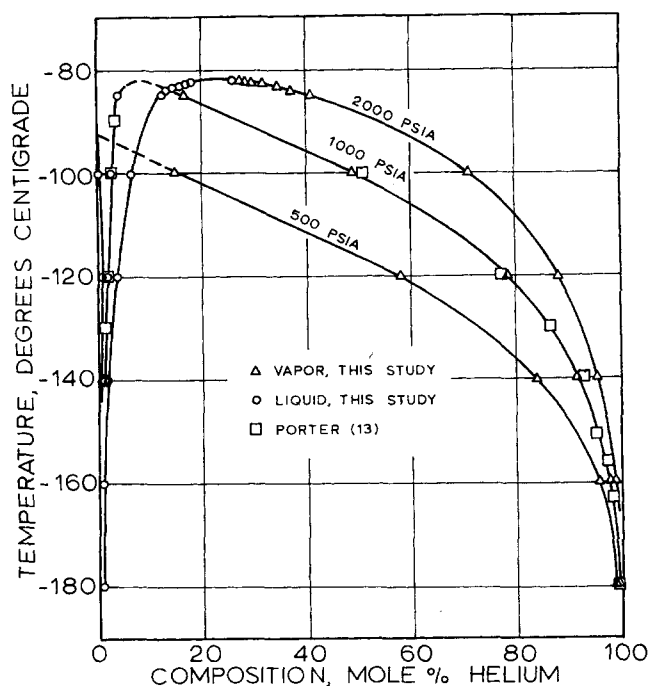


Fig. 2. Isobaric temperature-composition diagram, helium-methane.

A more detailed description of the experimental equipment and procedures is available (11).

## EXPERIMENTAL RESULTS

Six different isotherms of the helium-methane system were investigated at  $-85^{\circ}$ ,  $-100^{\circ}$ ,  $-120^{\circ}$ ,  $-140^{\circ}$ ,  $-160^{\circ}$ , and  $-180^{\circ}\text{C}$ . The highest of these isotherms is less than  $3^{\circ}\text{C}$ . below the critical temperature of methane and the lowest is less than  $4^{\circ}\text{C}$ . above the normal melting point of methane. For each temperature, equilibrium phase concentrations were determined at intervals of 250 lb./sq. in. from the vapor pressure of methane to 2,000 lb./sq. in. abs. In addition, the 2,000 lb./sq.in.abs. isobar was extended to the critical temperature of the mixture. At least two samples were taken at each temperature and pressure and two chromatograph analyses made of each sample. Thus the results in Tables 1 and 2 represent an average of at least four chromatograph runs for each data point.

Since the data were taken at the same pressures along each isotherm, it is possible to present the experimental results directly, without interpolation, on both P-X (pressure-composition) and T-X (temperature-composition) diagrams. The P-X plot obtained for the liquid phase shows that at higher pressures, as with helium-nitrogen, the solubility of helium in liquid methane increases with temperature, a reverse-order solubility system. At lower pressures the solubility passes through a maximum value.

Both vapor and liquid phase compositions are plotted in the T-X diagram of Figure 2. At pressures below the critical pressure of methane, the liquid phase isobar and the vapor phase isobar must intersect the 0% helium axis at the temperature corresponding to the vapor pressure of the pure methane. In Figure 2 this is illustrated by the extrapolation of the 500 lb./sq. in. abs. vapor phase isobar, which intercepts the y axis at the same point as the 500 lb./sq. in. abs. liquid isobar. At high pressure, the locus of vapor and liquid compositions is a single, smooth, continuous curve, such as appears for the 2,000 lb./sq. in. abs. isobar. At intermediate pressures the curve must be approximately as shown for the 1,000 lb./sq. in. abs. isobar.

The behavior of the helium-methane system is seen to be very similar to that of the helium-nitrogen system, except that helium is much less soluble in methane than in nitrogen. Both systems exhibit the type of behavior shown in general by systems where one component is far above its critical temperature.

The data, plotted as either T-X or P-X diagrams, exhibit very little scatter about the smooth lines, the deviations being not much larger than the estimated accuracy of the analytical procedure. A major goal in obtaining these data was to establish the reliability of the previously published data of Kharakhorin. In Figure 3 a comparison is made of the two isotherms which are most nearly the same for the two studies. Two points are to be observed. First, Kharakhorin's data exhibit more scatter about a smooth curve. Second, the data of this investigation plot on a smooth curve passing through the observed vapor pressure of methane at 0% helium concentration. The comparison in Figure 3 is limited to only two isotherms for clearness in presentation. However, the same situation exists for all the liquid phase data. In all cases the data of this study are more internally consistent, indicate a lower concentration of helium in liquid methane, and extend smoothly through the methane vapor pressure.

The study by Gonikberg and Fastovskii covered only two isotherms and was limited to such low temperatures, with correspondingly low helium concentrations in the liquid, that no particularly meaningful comparisons could be made. Although their data show considerably better agreement with this study than with Kharakhorin's, the indicated solubility of helium is still higher than that obtained in this investigation.

Some fragmentary data for the helium-methane system were obtained by Porter in 1925 but were never published (13). Vapor and liquid compositions were obtained for a number of temperatures at approximately 1,000 lb./sq. in. abs. Porter's data show excellent agreement with the results of this study, as shown in Figure 2. The majority of his points fall within the experimental scatter from the smoothed lines.

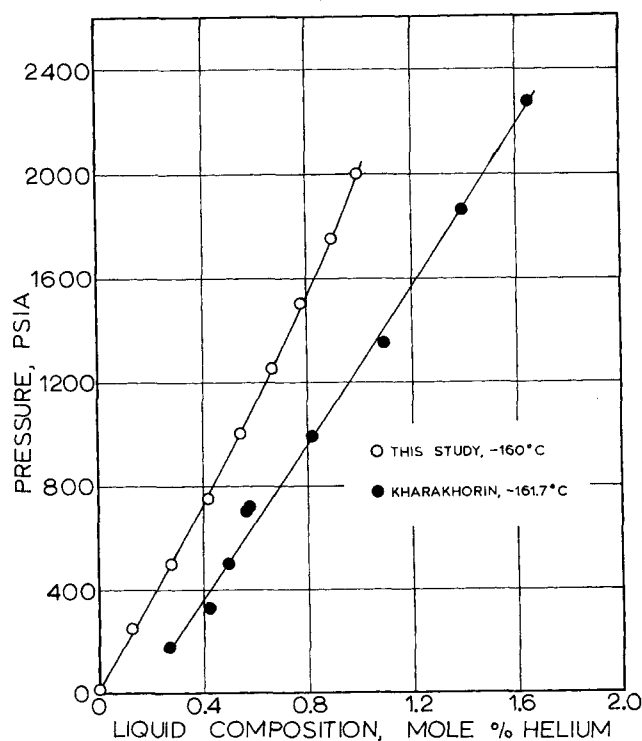


Fig. 3. Data comparison, helium-methane.

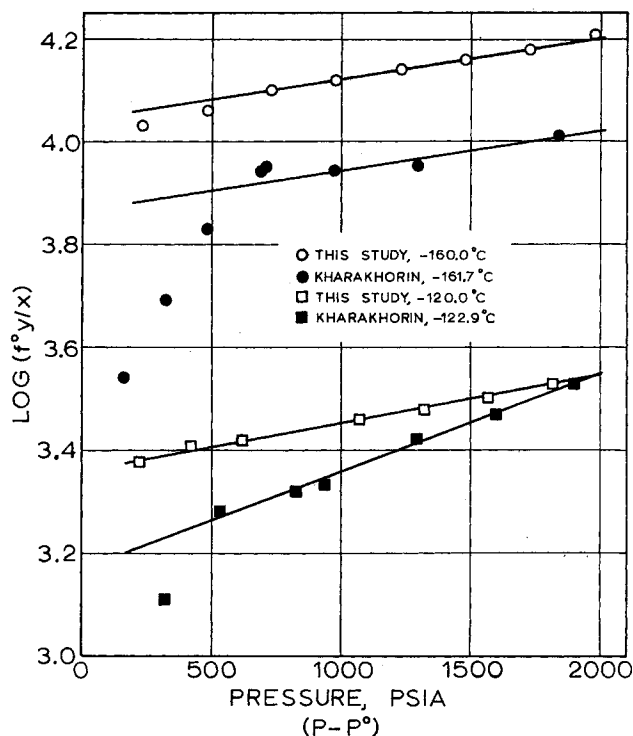


Fig. 4. Krichevsky-Kazarnovsky equation.

Kharakhorin, in a subsequent article (8), smoothed his data by means of the Krichevsky-Kazarnovsky equation (9):

$$\log (f/x)_1 = \log K + \bar{V}_1 (P - P_0) / (2.3 RT) \quad (1)$$

The left side of Equation (1) was evaluated from the Lewis and Randall fugacity rule  $f = f^0 y$  and plotted against  $(P - P_0)$ . If the partial molal volume is constant at a given temperature, a straight line with slope equal to the partial volume should result. This equation has proved useful in extrapolating  $y/x$  data to high pressures.

By using the fugacity values presented by Kharakhorin, Equation (1) was plotted for two isotherms from each

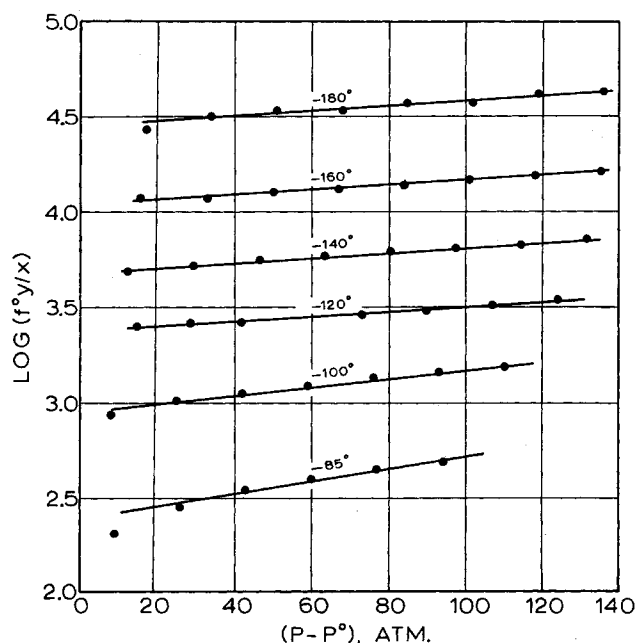


Fig. 5. Krichevsky-Kazarnovsky equation.

study in Figure 4. No specific conclusions were drawn directly from a study of Figure 4, other than the fact that the data from this study show less scatter about a straight line than do Kharakhorin's. In both cases deviations are observed at low pressures.

In order to extend the correlation over the complete temperature range covered by this investigation, it was necessary to compute the fugacity of pure helium in the range not considered by Kharakhorin. Fugacities were calculated by graphical integration of the equation

$$\ln (f/P) = \int_0^P (V/RT - 1/P) dP \quad (2)$$

Data for the specific volume of helium are available from the National Bureau of Standards (12). Although these data do not extend to the highest pressures reached in this study, they may be easily extrapolated, because the integrand in Equation (2) is practically constant with pressure. The calculated fugacities differed somewhat from Kharakhorin's values. This is probably due to the fact that he used a less exact equation of state based on fewer data than did the Bureau of Standards. Figure 5 contains the plots of Equation (1) for all six isotherms. A comparison of the  $-160^\circ\text{C}$ . isotherm with the same isotherm in Figure 4 indicates that at least some of the nonlinearity evident at low pressures in Kharakhorin's data is due to the fugacity calculations.

The data in Figure 5 indicate that Equation (1) could be satisfactorily used to extrapolate the data of this study to higher pressures if desired.

## CONCLUSIONS

New vapor-liquid equilibrium data have been presented for the helium-methane system. The data are more extensive than previously published data in the literature and are believed to be more accurate. The solubility of helium in liquid methane was found to be lower than that indicated by earlier studies. The data can easily be extrapolated to even higher pressures.

## ACKNOWLEDGMENT

This investigation was supported by Grant NSF GP-386 from the National Science Foundation. The methane was furnished through the courtesy of Phillips Petroleum Company and the helium by the Helium Research Center, U. S. Bureau of Mines. Financial aid through fellowships from Cities Service Oil Company and North American Aviation is also gratefully acknowledged.

## NOTATION

$f$	= fugacity
$K$	= Henry's law constant
$P$	= pressure
$R$	= perfect gas law constant
$T$	= temperature
$V$	= molal volume
$\bar{V}$	= partial molal volume
$x$	= mole fraction, liquid phase
$X$	= mole fraction
$y$	= mole fraction, vapor phase

## Subscripts

1	= component 1, lighter component
2	= component 2, heavier component

## Superscript

$o$	= pure component value
-----	------------------------

## LITERATURE CITED

1. Buzyna, George, R. A. Macriss, and R. T. Ellington, *Chem. Eng. Progr. Symposium Series No. 44*, **59**, 101 (1963).
2. DeVaney, W. E., B. J. Dalton, and J. C. Meeks, *J. Chem. Eng. Data*, **8**, 473 (1963).
3. Fedoritenko, A., and M. Ruehmann, *Tech. Phys. (USSR)*, **4**, 36 (1937).
4. Gonikberg, M. G., and W. Fastovskii, *Acta Physicochim. (USSR)*, **12**, 67 (1940).
5. ———, *Foreign Pet. Technol.*, **9**, No. 6, 214 (1941).
6. Kharakhorin, F. F., *J. Tech. Phys. (USSR)*, **10**, 1533 (1940).
7. ———, *Inz.-Fiz. Z.*, **2**, No. 5, 55 (1959).
8. *Ibid.*, No. 9, 24 (1959).
9. Krichevsky, I. R., and J. S. Kasarnovsky, *J. Am. Chem. Soc.*, **57**, 2168 (1935).
10. Rodewald, N. C., J. A. Davis, and Fred Kurata, *A.I.Ch.E. J.*, **10**, 937 (1964).
11. Sinor, J. E., Ph.D. thesis, Univ. Kansas, Lawrence (1965).
12. U. S. Natl. Bureau Standards Tech. Note 154, Dept. Commerce (1962).
13. "Open File of Information and Data Relating to the Extraction of Helium from Natural Gas by Low Temperature Processes," U. S. Bureau Mines, Amarillo, Tex. (1959).

Manuscript received August 2, 1965; revision received November 11, 1965; paper accepted November 15, 1965.

# Viscosity Profiles, Discharge Rates, Pressures, and Torques for a Rheologically Complex Fluid in a Helical Flow

J. G. SAVINS and G. C. WALLICK

Socony Mobil Oil Company, Inc., Dallas, Texas

Quantitative predictions are presented to show how the axial discharge rate and pressure gradient and angular velocity and torque become coupled when a fluid exhibiting a shear-dependent viscosity behavior is subjected to a helical flow field. The numerical scheme developed here is completely general and applicable to a wide choice of constitutive equations. For purposes of illustration only, results are described for an Oldroyd type of constitutive equation. The coupling effect is illustrated for different relative speeds of the cylinders, axial flow rates, axial pressure gradients, and ratios of cylinder diameters. The most interesting consequence of the coupling effect is that the axial flow resistance is lowered in a helical flow with the result, for example, that for a given applied axial pressure gradient, the axial discharge rate in a helical flow field is higher than in a purely annular flow field.

Helical flow is a steady flow which can occur when an annular mass of fluid is contained between two coaxial cylinder of radii  $R_i$  and  $R$  ( $R > R_i$ ) which rotate about their common axis with angular velocity  $\Omega_i$  and  $\Omega$ , respectively, and a constant pressure gradient  $J$ , parallel to the axis of the cylinders, is impressed on the fluid. In a helical flow each particle describes a path about the axis of the cylinders with an angular velocity  $\omega$  about the axis and a velocity  $u$  parallel to it,  $\omega$  and  $u$  being functions of  $r$  only, the radial distance of the particle from the axis of the cylinders.

This multidimensional flow field is of particular interest to the experimental rheologist, since it includes as special cases each of the other viscometric flow problems for which exact solutions are known for incompressible fluids: Poiseuille flow, flow between concentric pipes, that is, annular flow, of which channel flow is a special case, and Couette flow. In principle if measurements from a given

viscometric flow experiment are combined with the expressions for the stresses and the velocities to determine the material functions for, say, the *simple fluid* (1) or the material constants for the Oldroyd types of equations (2), then complete stress and velocity profiles can be predicted for helical flow or any of the other viscometric flows. A variety of treatments of the helical flow problem for rheologically complex fluids is to be found in the literature. Rivlin (3) introduced the term *helical flow* in a discussion of this superposition of annular and Couette flows for fluids of the differential type. However, he did not solve the resulting equations for the discharge rate and torque in terms of the applied pressure gradient, relative rotational speed, and rheological parameters. Coleman and Noll (4) derived such expressions. Fredrickson (5) used the constitutive equation devised by Rivlin, introducing a function which turns out to be simply the shear dependent viscosity function  $\eta$ . Coleman and Noll used the